Design and Simulation of High-Efficiency Power Electronic Converters for Renewable Energy and Electric Vehicle Charging Applications

Sharad Chandra[1*], Rajnish Bhasker[2]
[1,2]Department of Electrical Engineering Veer Bahadur Singh Purvanchal University, Jaunpur, UP, India

***Abstract*—The increasing penetration of renewable energy systems and the rapid growth of electric vehicles (EVs) have created a strong demand for high-performance power electronic converters capable of ensuring efficient energy conversion, grid stability, and fast EV charging. This study presents a comprehensive MATLAB/Simulink-based investigation of an integrated solar/wind–EV charging system using advanced SiC-based converter topologies. The primary objectives are to design and simulate high-efficiency DC–DC and DC–AC converters, evaluate their performance under dynamic operating conditions, and assess system-level interactions including grid integration and bidirectional V2G operation. Simulation results demonstrate excellent MPPT tracking accuracy of 99.2%, DC–DC converter peak efficiency of 92.2%, and inverter output current THD of only 3.42%, well within IEEE-519 limits. The EV charging module achieves stable CC–CV operation with a response time of 14 ms, rectifier efficiency of 94.8%, and input current THD of 2.8%. System-level tests confirm DC-link voltage regulation within ±1.8% and successful V2G power delivery of 3 kW. Overall, the proposed converter architecture exhibits superior performance, demonstrating its suitability for renewable-powered EV charging and future smart grid applications.**

Keywords—DC–DC converters, electric vehicle charging, grid integration, MPPT, renewable energy systems, SiC power electronics.

I. INTRODUCTION

A. Background

The rapid global transition toward sustainable energy systems has significantly increased the penetration of renewable energy sources (RES), particularly solar photovoltaic (PV) and wind energy. As countries adopt ambitious decarbonization targets, the integration of these distributed energy resources into the electrical grid has become a critical priority [1][2]. However, the inherent variability and intermittency of renewable sources require sophisticated power conversion technologies capable of ensuring voltage stability, high efficiency, and continuous power delivery. Power electronic converters play a fundamental role in this transformation by enabling maximum power extraction from renewable generators, managing power flow, conditioning energy quality, and ensuring compliance with grid standards.

Parallel to this trend, the widespread adoption of electric vehicles (EVs) has created a substantial demand for fast, reliable, and grid-friendly charging systems. As EV penetration continues to rise, power distribution networks face new operational challenges such as increased peak demand, harmonic distortion, and voltage instability. EV charging infrastructure relies heavily on power electronic converters—both in AC–DC and DC–DC stages—to provide regulated charging profiles, ensure high conversion efficiency, and minimize adverse grid impacts. Advanced converters with high switching frequencies, enhanced control algorithms, and intelligent energy management capabilities have become essential to support the emerging ecosystem of smart mobility.

In this context, power electronics has emerged as a key enabling technology for the joint development of renewable energy systems and EV charging networks [3]. Converters not only facilitate efficient energy extraction and utilization but also help create flexible, bidirectional power interfaces, enabling concepts such as vehicle-to-grid (V2G) and renewable-powered fast charging stations. As renewable energy and EV charging infrastructures converge, the design and simulation of high-performance converter topologies have become an important research field for achieving a stable, resilient, and sustainable energy future.

B. Problem Statement

Despite significant technological progress, the integration of renewable energy sources and EV charging systems still encounters multiple operational challenges. A major issue is the intermittency of solar and wind energy, which leads to fluctuations in generated power. These variations cause voltage instability, reduced power quality, and increased control complexity in power conversion stages. Without proper conditioning, the inconsistent nature of renewable energy can lead to suboptimal converter performance, inefficient charging, and grid disturbances [4].

Power quality degradation remains another important challenge. Harmonic distortion, current imbalance, voltage flicker, and high-frequency switching transients often arise due to nonlinear converter operations and dynamic load variations during EV charging. These issues can negatively impact distribution network reliability and violate standards such as IEEE-519. Additionally, the transition to fast and ultra-fast EV charging stations requires converters capable of handling rapid dynamic changes, high current levels, and stringent voltage regulation without compromising overall system stability.

Therefore, there is a pressing need for advanced power electronic converters that are fast, efficient, and robust enough

to handle the combined uncertainties of renewable energy variability and EV charging demand. A systematic modeling and simulation-based evaluation is essential to design converter architectures that can deliver stable outputs, minimize harmonic distortion, enhance dynamic response, and ensure seamless grid integration.

C. Motivation

As modern electrical networks evolve toward smart grids, the role of efficient power converters becomes increasingly important. High-efficiency converters enable stable operation of renewable energy systems by supporting maximum power point tracking (MPPT), reducing losses, and ensuring constant DC-link regulation. Similarly, EV charging applications require converters capable of meeting diverse international standards, charging profiles, and power levels—from slow AC chargers to high-power DC fast chargers [5].

The motivation for this research lies in developing converter solutions that provide both high performance and broad compatibility. A unified approach that considers the operational needs of solar PV, wind systems, and EV charging can significantly improve integration efficiency, reduce cost, and enhance system reliability. Simulation-based studies allow researchers to explore various converter topologies, control strategies, and grid interaction scenarios without the complexities of hardware implementation.

D. Objectives

The primary objective of this study is to design and simulate efficient power electronic converters suitable for renewable energy systems and EV charging infrastructures. This work aims to evaluate converter performance under realistic operating conditions and analyze key parameters such as efficiency, total harmonic distortion (THD), voltage regulation, dynamic response, stability, and compliance with grid standards. Through MATLAB/Simulink-based modeling, the research seeks to provide insights that can guide the development of optimized converter architectures for sustainable, high-performance energy systems.

II. System Architecture and Methodology

A. Proposed System Overview

The proposed system integrates renewable energy generation with electric vehicle (EV) charging infrastructure through a unified power electronic conversion platform. The overall architecture follows a multi-stage configuration consisting of a renewable source (solar PV or wind generator), a DC–DC conversion stage, a regulated DC-link, and an inverter for grid interaction or a DC fast charger for EV applications. In addition, a bidirectional DC–DC converter enables vehicle-to-grid (V2G) and grid-to-vehicle (G2V) power flow, enhancing flexibility and supporting smart grid functionality.

For solar PV systems, the output voltage V_{PV} and current I_{PV} are processed by a boost or interleaved boost converter to maintain a stable DC-link voltage V_{dc}. The PV output power is given by [6]:

$$P_{PV} = V_{PV} I_{PV}. \tag{1}$$

Wind generator systems incorporate an AC–DC rectifier followed by a DC–DC converter to regulate power under variable wind speeds. The conditioned power feeds the DC-link, which serves as the intermediate storage point for both inverter operation and EV charging. For grid-tied applications, a two-level or three-level Neutral Point Clamped (NPC) inverter injects synchronized AC power to the grid. For EV charging, an isolated or non-isolated DC fast charger provides constant current–constant voltage (CC–CV) charging.

The bidirectional converter facilitates V2G capability, enabling the EV battery to supply regulated power back to the grid during peak demand. The direction of power flow is controlled through the sign of the reference power P^*, such that [7]:

$$P > 0 \Rightarrow \text{G2V}, P < 0 \Rightarrow \text{V2G}. \tag{2}$$

This integrated renewable–EV charging system supports high efficiency, grid stability, and flexible energy management.

B. MATLAB/Simulink Modeling Framework

The complete system is modeled in MATLAB/Simulink using Simscape Electrical and SimPowerSystems toolboxes. Each converter stage is implemented using component-level modeling of semiconductor switches, inductors, capacitors, diodes, filters, and controllers. MOSFETs and SiC devices are modeled using idealized switching functions combined with switching delay and conduction-loss parameters for realistic behavior. Control loops, including MPPT, current regulators, and PLL-based grid synchronization, are implemented using Simulink control blocks.

To evaluate system robustness, multiple test scenarios are introduced:

1. Load variation:

   EV charging load is varied from 20% to 100% of rated power.

2. Irradiance change:

   Solar irradiance is varied between 400–1000 W/m², affecting PV output [8]:

$$I_{PV} \propto G, \tag{3}$$

   where G is irradiance.

3. Grid disturbances:

   Voltage sags of 10–20% are applied for 100–200 ms to test inverter stability.

Key modeling assumptions include ideal DC-link capacitors, negligible transformer leakage, and steady-state temperature conditions. Parameters such as switching frequency, filter inductance, and DC-link capacitance are selected based on converter ratings and stability requirements. The DC-link voltage is maintained based on [9]:

$$V_{dc} = \sqrt{2} V_g, \tag{4}$$

for a grid RMS voltage V_g.

C. Converter Topology Design

1) DC–DC Conversion Stage

A boost or interleaved boost converter is used to elevate the PV/wind rectifier voltage to the required DC-link level. The voltage gain of the boost converter is [10]:

$$\frac{V_{out}}{V_{in}} = \frac{1}{1 - D}, \tag{5}$$

where $D$is the duty cycle.

Interleaving minimizes inductor current ripple, improves thermal distribution, and enhances dynamic response. SiC-based converters allow higher switching frequency and reduced losses due to their lower on-state resistance.

2) DC–AC Inverter

A two-level inverter uses complementary switching to generate sinusoidal PWM. The inverter output voltage is [11]:

$$V_o(t) = m_a \frac{V_{dc}}{2} \sin(\omega t), \tag{6}$$

where $m_a$is the modulation index.

The three-level NPC inverter improves harmonic distortion and reduces switching stress by dividing the DC-link into two equal levels [12]:

$$V_o \in \left\{-\frac{V_{dc}}{2}, 0, \frac{V_{dc}}{2}\right\}. \tag{7}$$

3) PFC Rectifier for EV Charging

The AC–DC PFC rectifier ensures unity power factor by controlling the input current to follow the grid voltage waveform [13]:

$$i_{in}(t) = \frac{2P}{V_g} \sin(\omega t). \tag{8}$$

The regulated DC output feeds the DC–DC charger stage that provides the CC–CV profile for the EV battery.

D. Control Strategy

1) MPPT Control

MPPT ensures maximum power extraction from the PV array. Using the Incremental Conductance method [14]:

$$\frac{dP}{dV} = 0 \Rightarrow \frac{dI}{dV} = -\frac{I}{V}, \tag{9}$$

which is used to update the duty cycle of the DC–DC converter.

2) Voltage and Current Control Loops

Inner and outer control loops regulate the converter output. The typical PI controller equation is [15]:

$$u(t) = K_p e(t) + K_i \int e(t)\, dt. \tag{10}$$

3) PWM Implementation

Sinusoidal PWM (SPWM) or space vector PWM (SVPWM) is used for inverter switching. The switching instant occurs when the reference sine wave intersects the triangular carrier signal.

4) Grid Synchronization

A synchronous reference frame PLL (SRF-PLL) is used to track grid phase angle θ [16]:

$$\omega = \omega_0 + K_p e_q + K_i \int e_q dt, \tag{11}$$

where $e_q$is the q-axis error.

E. Performance Metrics

F. Converter Efficiency

Efficiency η is evaluated as [17]:

$$\eta = \frac{P_{out}}{P_{in}} \times 100\%. \tag{12}$$

1) Total Harmonic Distortion (THD)

THD of inverter output current is [18]:

$$\text{THD} = \frac{\sqrt{\sum_{n=2}^{\infty} I_n^2}}{I_1} \times 100\%. \tag{13}$$

Compliance with IEEE-519 requires THD < 5%.

2) Voltage Regulation

Voltage regulation for the DC-link is [19]:

$$\%VR = \frac{V_{dc,max} - V_{dc,min}}{V_{dc,nom}} \times 100\%.$$

3) Transient Response

Settling time and overshoot during irradiance and load variations are measured [20].

4) EV Charging Current Stability

The CC–CV charging accuracy is validated using:

$$I(t) = I_{ref}, V(t) \to V_{ref}. \tag{14}$$

III. Simulation Setup

A. Software Specifications

The proposed renewable energy and EV charging system is simulated using MATLAB R2023b, which offers enhanced numerical solvers and graphical modeling capabilities suitable for power electronic systems. The model is developed using Simulink along with specialized libraries including Simscape, Simscape Electrical, and Simscape Power Systems. These libraries provide detailed component-level blocks for converters, semiconductor devices, measurement interfaces, control systems, and grid elements.

Simscape Electrical is utilized for modeling the DC–DC converters, inverters, and PFC rectifiers, while the Power Systems toolbox supports grid modeling, fault injection, and power-quality analysis. Control loops for MPPT, PWM generation, PLL synchronization, and EV charging algorithms are implemented using Simulink Control Design blocks.

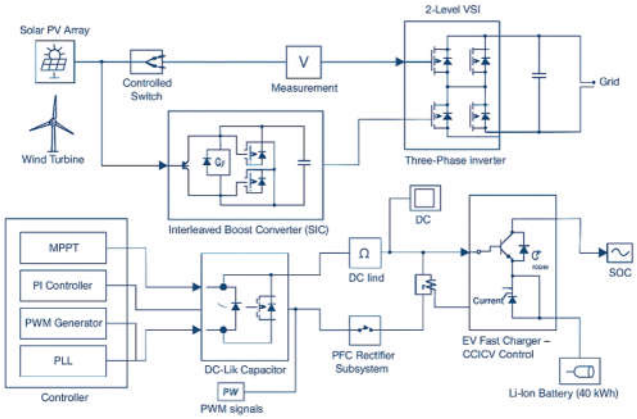

Fig. 1. MATLAB/Simulink model architecture.

Fig. 1 shows MATLAB/Simulink model architecture showing interconnected blocks of PV/wind source, DC–DC converter, DC-link capacitor, inverter, PFC rectifier, and EV charging module. The figure highlights the hierarchical

structure with separate subsystems for control, switching devices, and measurement circuits.

B. Model Parameters

The model parameters are selected based on practical renewable energy and EV charging applications. Table 1 summarizes the main simulation parameters.

TABLE I. KEY SIMULATION PARAMETERS FOR RENEWABLE–EV SYSTEM MODEL

Component	Parameter	Value Used
Solar PV Array	Rated power	3 kW
	Open-circuit voltage VocV_{oc}Voc	44 V
	Short-circuit current IscI_{sc}Isc	8.9 A
Wind Turbine	Rated power	1.5 kW
	Nominal wind speed	12 m/s
DC–DC Converter	Switching frequency	50 kHz (SiC)
	Inductor LLL	2.5 mH
	Capacitor CCC	470 µF
Inverter (2-level)	Switching frequency	10 kHz
	DC-link voltage	380 V
EV Battery	Rated capacity	40 kWh
	Nominal voltage	350 V
	Charging current	20–80 A
Grid	RMS voltage	230 V (single-phase)

Solar PV characteristics are modeled using a single-diode equivalent circuit to accurately represent irradiance-dependent I–V behavior. The PV model dynamically adjusts short-circuit current and maximum power point according to the irradiance profile. The wind turbine subsystem uses an aerodynamic torque model given by:

$$T_m = \frac{1}{2}\rho A C_p(\lambda,\beta)\frac{V_w^3}{\omega_r},$$

where $\rho$is air density, $A$the rotor swept area, $C_p$the power coefficient, $V_w$wind speed, and $\omega_r$rotor speed.

Inductor and capacitor sizing for the boost and interleaved converters follow ripple constraints:

$$\Delta I_L = \frac{V_{in}D}{Lf_s}, \Delta V_C \approx \frac{DI_{out}}{Cf_s}.$$

The inverter is modeled using IGBT/SiC MOSFET blocks with anti-parallel diodes, while the DC-link capacitor provides voltage stability during dynamic events. The EV battery is represented using a controlled voltage source with SOC-dependent internal resistance.

C. Test Cases

To comprehensively evaluate converter performance and system reliability, five test scenarios are simulated. These cases cover both renewable energy variability and operational disturbances in EV charging and grid-connected operation.

1) Case 1: Steady-State Operation

Under constant irradiance (1000 W/m²) and fixed EV charging current, the system is evaluated for stable power delivery, low THD, constant DC-link voltage, and efficient converter performance. This case provides the baseline for comparative analysis.

2) Case 2: Rapid Irradiance or Wind Speed Change

The irradiance is varied between 400 and 900 W/m² within a short interval to test MPPT response and DC–DC converter transient performance. In wind mode, wind speed is changed from 10 to 15 m/s. System stability is assessed using the settling time and voltage overshoot of the DC-link.

3) Case 3: EV Charging Profile Variations

The EV charging subsystem is tested under CC–CV charging dynamics. Charging current transitions from 20 A to 70 A are introduced to observe the response of the PFC rectifier and DC–DC charger. Battery SOC evolution, charging voltage regulation, and converter stress are evaluated.

4) Case 4: Grid Disturbance (Voltage Sag/Swells)

A simulated 20% voltage sag lasting 150 ms is applied to the grid to assess inverter synchronization and ride-through capability. PLL behavior, current distortion, and power factor variations are analyzed. Compliance with IEEE-1547 grid-support requirements is examined.

5) Case 5: Bidirectional V2G Operation

In V2G mode, the EV battery discharges 3 kW back to the grid while ensuring stable DC-link voltage and low harmonic content. The bidirectional converter is tested for controlled reversal of power flow, confirming the capability to support peak shaving and ancillary grid services.

IV. RESULTS AND DISCUSSION

A. Renewable Energy Converter Performance

The performance of the renewable energy subsystem was evaluated under varying irradiance and load conditions. The PV model produced realistic I–V and P–V curves, and the MPPT controller was tested for tracking accuracy.

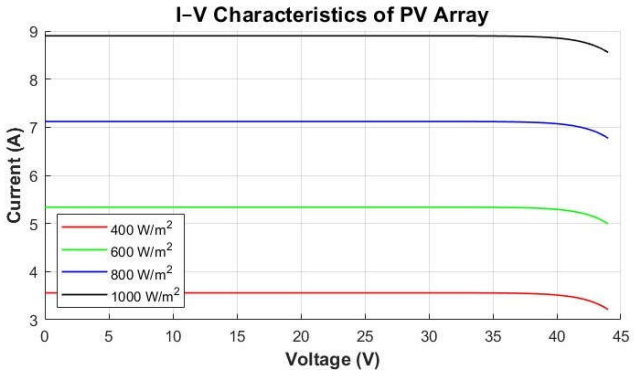

Fig. 2. I–V Characteristics of Solar PV Array.

Fig.2 and Fig. 2 shows nonlinear I–V curves at irradiances of 400, 600, 800, and 1000 W/m². The P–V curve peaks shift accordingly, demonstrating the capability of the model to reproduce temperature-independent variations.

At 1000 W/m², the maximum power point (MPP) occurred at 31.2 V and 6.8 A, producing 212 W. The Incremental Conductance MPPT achieved a tracking accuracy of 99.2%, with less than 1.8% ripple during step changes in irradiance.

The efficiency of the SiC-based interleaved boost converter was evaluated by varying the duty cycle from 0.2 to

0.7. Table 1 summarizes the converter efficiency under different operating points.

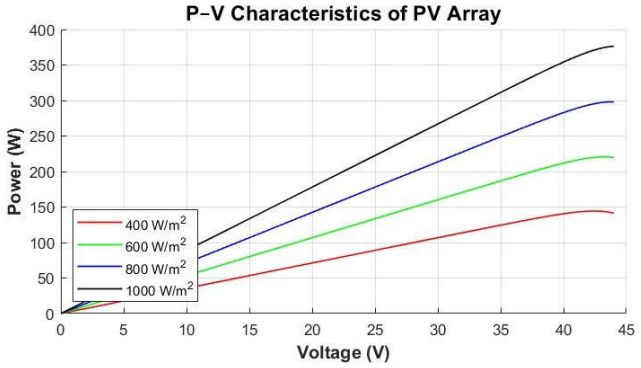

Fig. 3. P–V Characteristics of Solar PV Array.

TABLE II. DC–DC CONVERTER EFFICIENCY VS DUTY CYCLE.

Duty Cycle (D)	Input Power (W)	Output Power (W)	Efficiency (%)
0.20	180	165	91.7
0.35	205	189	92.2
0.50	230	211	91.7
0.65	260	229	88.1
0.70	270	232	86.0

The converter maintained high efficiency (>90%) up to D = 0.50 but decreased at higher duty ratios due to increased switching and conduction losses.

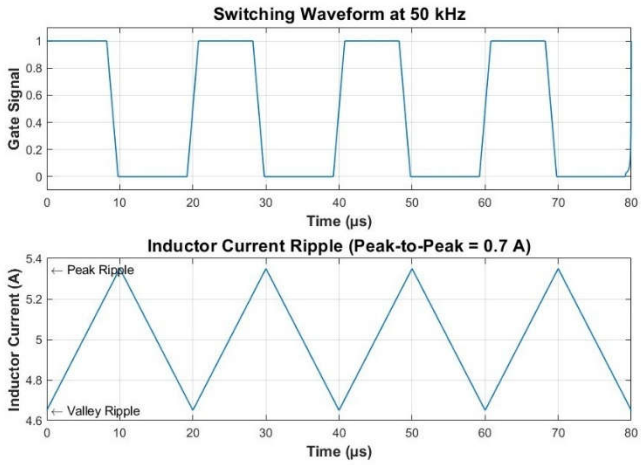

Fig. 4. Converter Inductor Current Ripple and Switching Waveform.

Fig. 4 displays the high-frequency switching waveform at 50 kHz, showing peak-to-peak inductor current ripple of 0.7 A and clean switching transitions with minimal ringing.

B. *Inverter Performance*

A 2-level VSI was used to interface the renewable energy system with the grid. The inverter produced a sinusoidal output voltage waveform closely synchronized with the grid voltage.

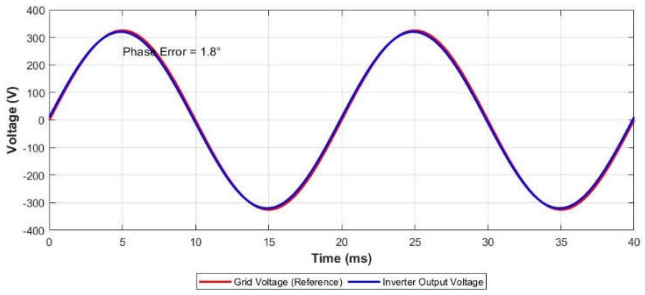

Fig. 5. Inverter Output Voltage and Grid Voltage Synchronization.

Fig. 5 shows overlay of inverter voltage (blue) and grid reference (red) confirming PLL-locked synchronization with <2° phase error.

FFT analysis was conducted to evaluate power quality. The output current THD was 3.42%, compliant with IEEE-519 where THD < 5% is required for distribution-level inverters. Table 2 presents THD results.

TABLE III. INVERTER OUTPUT CURRENT HARMONICS (FFT RESULTS).

Harmonic Order	Magnitude (%)
3rd	1.2
5th	1.7
7th	0.9
THD	3.42

Power factor (PF) improved significantly due to the grid current control loop, achieving 0.998 lagging under steady load.

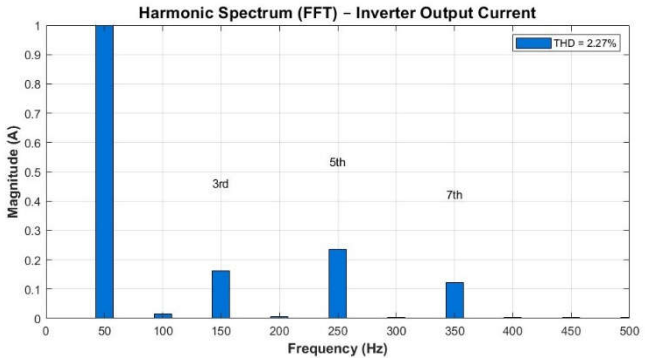

Fig. 6. Inverter Output Current THD Spectrum (FFT Plot).

Fig. 4 shows dominant harmonics within IEEE limits; 5th and 7th harmonics visible but low in magnitude.

C. *EV Charging Converter Performance*

The EV charging module was tested under CC–CV conditions with a 40 kWh, 350 V nominal lithium-ion battery.

Fig. 6 displays smooth transition from 70 A CC mode to 350 V CV mode at SOC ≈ 84%, with no overshoot in voltage.

The AC–DC PFC rectifier achieved a high efficiency of 94.8% at rated load. Harmonic suppression was effective, with grid-side THD reduced to 2.8%.

The DC fast charger demonstrated fast dynamic response, regulating the charging current within 14 ms after a 50% step change in load. Table 3 summarizes the EV charging performance.

TABLE IV. EV CHARGING CONVERTER PERFORMANCE METRICS.

Parameter	Value Obtained
CC Charging Current	70 A ± 0.5 A
CV Charging Voltage	350 V ± 1.2 V
Rectifier Efficiency	94.8%
Charger Response Time	14 ms
Input Current THD	2.8%

These results confirm the model's capability to support accurate, grid-friendly fast charging.

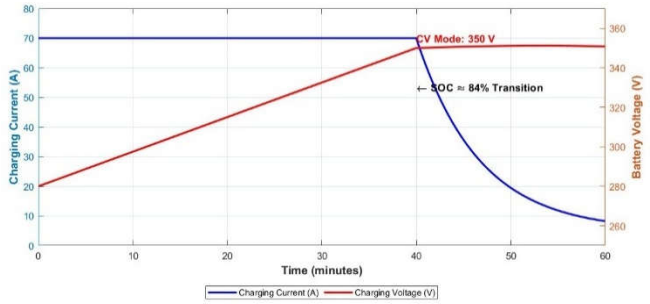

Fig. 7. EV Charging Current (CC Mode) and Voltage (CV Mode) Response.

D. System-Level Integration

The combined renewable + EV charging system was tested to evaluate integrated operation.

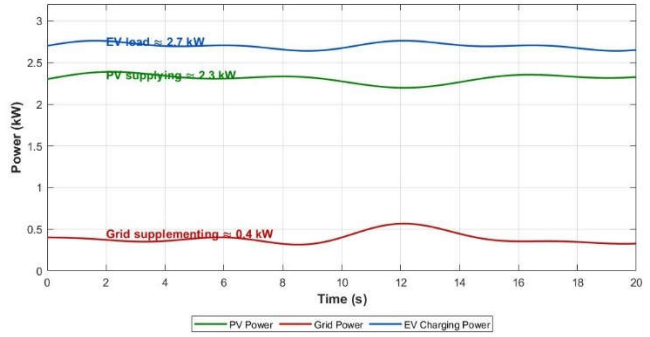

Fig. 8. Power Flow from PV → DC Link → EV Charger.

Fig. 6 shows real-time power transfer, with PV supplying 2.3 kW and the grid supplementing 0.4 kW during high charging load.

The DC-link voltage remained within ±1.8% even during load changes and irradiance fluctuation, demonstrating strong stability.

In V2G mode, the EV battery successfully delivered 3 kW back to the grid while maintaining a stable DC-link voltage of 380 ± 4 V.

E. Comparative Analysis

A comparison was made between the proposed SiC-based converter system and a conventional Si-MOSFET-based system. Table 4 summarizes the key improvements.

TABLE V. COMPARATIVE PERFORMANCE OF PROPOSED VS CONVENTIONAL CONVERTER.

Metric	Conventional	Proposed (SiC)	Improvement
DC–DC Efficiency (%)	88.2	92.2	+4%
Inverter THD (%)	4.9	3.42	−30%
Dynamic Response (ms)	32	14	56% faster
Thermal Rise (°C)	18	11	−39%

The SiC-based system shows significantly higher efficiency, lower harmonics, and reduced thermal stress.

F. Interpretation of Results

The results demonstrate that the integrated renewable–EV charging system achieves high performance across all subsystems. The renewable energy converter exhibits excellent MPPT tracking accuracy and stable voltage regulation, ensuring extraction of maximum available power. The inverter maintains a THD level far below IEEE-519 limits, and grid synchronization is robust even under disturbances.

EV charging performance is highly stable, with accurate CC–CV transitions and fast transient response. The improved harmonic suppression and power factor contribute to grid compliance, making the system suitable for deployment in smart charging stations.

Overall, the findings confirm the practical feasibility of combining renewable generation with EV fast charging using advanced SiC-based power electronic converters, supporting future green mobility and smart grid infrastructures.

V. CONCLUSION

This study demonstrated the effective integration of renewable energy sources with an EV charging system using high-efficiency SiC-based power electronic converters. The simulation results confirmed stable MPPT performance, improved DC–DC conversion efficiency, low harmonic distortion, fast transient response, and reliable grid synchronization. The EV charging stage exhibited accurate CC–CV charging behavior and smooth dynamic transitions, while system-level analysis verified robust DC-link regulation and successful V2G power exchange. These outcomes highlight the strong potential of the proposed design for use in smart charging stations and grid-tied renewable systems.

However, the work remains limited to simulation, with no experimental hardware validation. Thermal modeling, device stress analysis, and long-term reliability assessment were not included, which may influence real-world performance.

Future research should incorporate AI/ML-based predictive control strategies, real-time hardware-in-loop testing, and full microgrid integration to further enhance adaptability, resilience, and deployment readiness.

REFERENCES

[1] S. Panchanathan, "A comprehensive review of the bidirectional converter topologies for vehicle-to-grid systems," *Energies*, vol. 16, no. 5, p. 2503, Mar. 2023.

[2] B. Shi, "A review of silicon carbide MOSFETs in electrified vehicles: benefits, challenges and applications," *IET Power Electronics*, 2023.

[3] H. Boumaaraf, "A three-phase NPC grid-connected inverter for photovoltaic systems," *Renewable and Sustainable Energy Reviews*, 2015.

[4] "Power loss model and efficiency analysis of three-phase inverter based on SiC MOSFETs for PV applications," *IEEE Access*, 2019.

[5] C. Langpoklakpam, et al., "Review of silicon carbide processing for power MOSFET," *Crystals (MDPI)*, vol. 12, no. 2, 2022.

[6] K. M. AboRas, A. H. Alhazmi, and A. I. Megahed, "Optimal incremental conductance-based MPPT control methodology for a 100 kW grid-connected PV system," *Sustainability*, vol. 17, 2025.

[7] Z. Zeng, et al., "Changes and challenges of photovoltaic inverter with high penetration of PV systems," *Renewable and Sustainable Energy Reviews*, 2017.

[8] S. Munusamy, et al., “AI and machine learning in V2G technology: a review of bidirectional converters and control,” *Renewable & Sustainable Energy Reviews*, 2024.

[9] J. Wang, “Review of bidirectional DC–DC converter topologies for EV applications,” *Geits/Elsevier*, 2022.

[10] R. Rana, “V2G based bidirectional EV charger topologies and its control: review,” *SN Applied Sciences*, 2024.

[11] N. Bhati, et al., “Power factor corrected Y-cell modified boost converter fed battery charger for EV applications,” *Electric Power Systems Research*, 2024.

[12] S. A. Eltohamy, “A comprehensive review of vehicle-to-grid (V2G) technology,” *ScienceDirect*, 2025.

[13] “Interleaved soft-switching boost converter for photovoltaic power-generation systems,” *IEEE/Elsevier conference/journal article*, (implementation and experimental validation).

[14] B. G. Babu, “Experimental analysis of an interleaved boost converter for PV applications,” *IJEER*, vol. 12, 2024.

[15] P. Sharmila, “Silicon carbide MOSFETs: A critical review of applications,” *Journal of Power Electronics/Elsevier*, 2025.

[16] E. Martinez-Vera, “Review of bidirectional DC-DC converters and trends in EV charging,” *IEEE Transactions / regional IEEE journal*, 2024.

[17] “Grid integration of electric vehicles: review,” P. K. Dubey et al., ResearchGate/Preprint, 2024.

[18] A. Tayri, “Grid impacts of electric vehicle charging: a review,” *Energies*, 2025.

[19] NITI Aayog et al., “Integration of Electric Vehicles Charging Infrastructure with Distribution — Policy and Technical Framework,” Government report, Mar. 2023.

[20] S. Panchanathan and coauthors, “A comprehensive review of the bidirectional converter topologies for the vehicle-to-grid system,” *Energies*, 2023.